

Article

Charge Transfer Complexes of 1,3,6-Trinitro-9,10-phenanthrenequinone with Polycyclic Aromatic Compounds

Roman Linko ^{1,*}, Michael Ryabov ¹, Pavel Strashnov ¹, Pavel Dorovatovskii ², Victor Khrustalev ^{1,3}  and Victor Davydov ¹

¹ Faculty of Science, Peoples' Friendship University of Russia (RUDN University), 6 Miklukho-Maklaya Street, 117198 Moscow, Russia; ryabov_ma@pfur.ru (M.R.); strashnov_pv@pfur.ru (P.S.); khrustalev_vn@pfur.ru (V.K.); davydov_vv@pfur.ru (V.D.)

² Kurchatov Complex for Synchrotron and Neutron Investigations, National Research Center "Kurchatov Institute", 123182 Moscow, Russia; paulgemini@mail.ru

³ N.D. Zelinsky Institute of Organic Chemistry, Russian Academy of Sciences, 119991 Moscow, Russia

* Correspondence: linko_rv@pfur.ru

Abstract: Understanding the interactions of organic donor and acceptor molecules in binary associates is crucial for design and control of their functions. Herein, we carried out a theoretical study on the properties of charge transfer complexes of 1,3,6-trinitro-9,10-phenanthrenequinone (PQ) with 23 aromatic π -electron donors. Density functional theory (DFT) was employed to obtain geometries, frontier orbital energy levels and amounts of charge transfer in the ground and first excited states. For the most effective donors, namely, dibenzotetraphiafulvalene, pentacene, tetrathiafulvalene, 5,10-dimethylphenazine, and tetramethyl-p-phenylenediamine, the amount of charge transfer in the ground state was shown to be 0.134–0.240 e^- . Further, a novel charge transfer complex of PQ with anthracene was isolated in crystalline form and its molecular and crystal structure elucidated by single-crystal synchrotron X-ray diffraction.

Keywords: charge transfer complex; DFT; X-ray diffraction; 1,3,6-trinitro-9,10-phenanthrenequinone; anthracene



Citation: Linko, R.; Ryabov, M.; Strashnov, P.; Dorovatovskii, P.; Khrustalev, V.; Davydov, V. Charge Transfer Complexes of 1,3,6-Trinitro-9,10-Phenanthrenequinone with Polycyclic Aromatic Compounds. *Molecules* **2021**, *26*, 6391. <https://doi.org/10.3390/molecules26216391>

Academic Editor: Jianzhang Zhao

Received: 29 September 2021

Accepted: 19 October 2021

Published: 22 October 2021

Publisher's Note: MDPI stays neutral with regard to jurisdictional claims in published maps and institutional affiliations.



Copyright: © 2021 by the authors. Licensee MDPI, Basel, Switzerland. This article is an open access article distributed under the terms and conditions of the Creative Commons Attribution (CC BY) license (<https://creativecommons.org/licenses/by/4.0/>).

1. Introduction

Organic π - π charge transfer complexes (CTCs) form a special class of binary compounds stabilized by partial electron transfer between noncovalently interacting donor (D) and acceptor (A) molecules. The degree of electron transfer in CTCs is governed by the difference between the donor ionization potential and the acceptor electron affinity which can be approximated as the difference between the donor highest occupied molecular orbital (HOMO) and the acceptor lowest unoccupied molecular orbital (LUMO) [1]. The HOMO-LUMO energy gap can be obtained from DFT calculations.

Individual CTCs may undergo self-assembly and form crystalline or supramolecular structures [2]. The properties of such assemblies depend on the stoichiometric composition of the complexes [3,4] and their polymorphism [5,6]. CTCs in crystals tend to form one of two types of molecular stacks: (a) mixed-type stacks with alternating donor and acceptor molecules $\{-D-A-D-A\}_\infty$ or $\{-D-A-D-D-A-D\}_\infty$ and (b) segregated stacks of donor and acceptor molecules $\{-D-D-D\}_\infty$ || $\{-A-A-A\}_\infty$ [3,7].

CTCs exhibit a wide range of physical properties therefore the search for new effective electron donors, acceptors, and synthesis of new CTCs on this basis is of high relevance [8]. At the same time, quantum-chemical modeling is one of the main approaches to study structure and properties of CTCs. Computer modeling allows a large number of complexes to be examined in a short period of time to select only a few of the most promising for further experimental research [9].

There have been only a few studies on CTCs with 9,10-phenanthrenequinone nitro derivatives as acceptors [10–12]. In [11,12], a series of CTCs based on anthracene, phenanthrene, and 9,10-phenanthrenequinone derivatives was studied. Of all the derivatives considered, 1,3,6-trinitro-9,10-phenanthrenequinone showed the strongest acceptor properties.

The purpose of the present work was to study CTCs based on 1,3,6-trinitro-9,10-phenanthrenequinone (PQ) as electron acceptor and different donors. We selected 23 donors with a varying number of π -electrons (from 6 to 26) and a different aromatic system structure; some of them had N and S heteroatoms and substituents. The following donors were used: benzene (BZ), pyridine (PD), N,N,N',N'-tetramethyl-p-phenylenediamine (TMDA), naphthalene (NA), quinoline (QN), isoquinoline (IQN), acenaphthene (ACN), azulene (AZU), tetrathiafulvalene (TTF), anthracene (AN), phenanthrene (PA), acridine (ACR), 9-methylcarbazole (MC), 5,10-dimethylphenazine (DMPZ), tetracene (TET), tetraphene (TPH), chrysene (CRS), pyrene (PYR), triphenylene (TPL), dibenzotetrathiafulvalene (DBTTF), pentacene (PEN), porphyrin (POR), coronene (COR) (Figure 1 and Supplementary Material Figure S1).

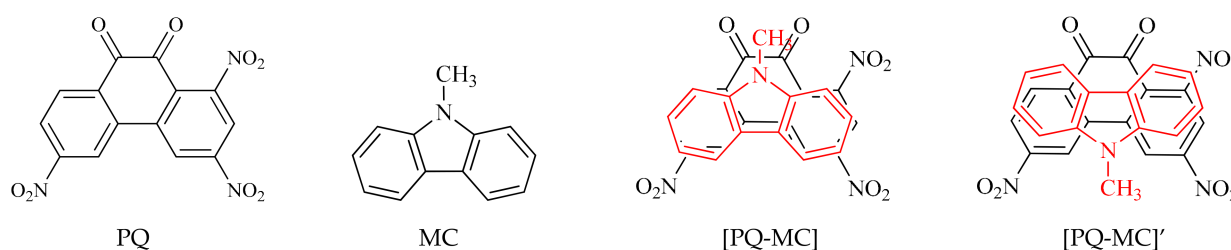


Figure 1. Configurations of acceptor PQ, one of the donors MC, and two possible CTCs [PQ-MC] and [PQ-MC]'.

Asymmetrical molecules such as PD, QN, IQN, PA, ACR, CCN, MC, TPH, and AZU produce different stable arrangements of donor and acceptor in CTCs, therefore, the quantum-chemical calculation was performed for 32 possible models (Figures 1 and S2, Table 1).

Table 1. The calculated energies (eV) of frontier molecular orbitals of donors and CTCs (D_{EHOMO} , $^{\text{CTC}}E_{\text{HOMO}}$, $^{\text{CTC}}E_{\text{LUMO}}$), energy gaps (eV) of isolated and interacting donor and acceptor (ΔE_{MO} , $\Delta ^{\text{CTC}}E_{\text{MO}}$), partial NPA charges (e^-) of complex ground and first excited states (q_{NPA} , q^*_{NPA}), and association energy (ΔE_{ass} , kJ/mol).

Molecule	D_{EHOMO}	ΔE_{MO}	$^{\text{CTC}}E_{\text{HOMO}}$	$^{\text{CTC}}E_{\text{LUMO}}$	$\Delta ^{\text{CTC}}E_{\text{MO}}$	q_{NPA}	q^*_{NPA}	ΔE_{ass}
[PQ-PD]	−6.97	2.40	−7.43	−3.92	3.51	0.138	0.080	−59.4
[PQ-Pd]'	−6.97	2.40	−7.61	−4.46	3.14	0.015	0.001	−46.6
[PQ-BZ]	−6.96	2.39	−7.50	−4.40	3.10	0.026	0.008	−47.0
[PQ-QN]	−6.53	1.96	−7.15	−4.35	2.79	0.019	0.071	−67.6
[PQ-Qn]'	−6.53	1.96	−7.06	−4.42	2.64	0.014	0.969	−63.3
[PQ-IQN]	−6.45	1.88	−7.01	−4.45	2.56	−0.003	0.971	−61.4
[PQ-IQn]'	−6.45	1.88	−7.05	−4.45	2.60	0.018	0.967	−64.2
[PQ-TPL]	−6.10	1.53	−6.58	−4.21	2.37	0.037	0.969	−106.5
[PQ-NA]	−6.04	1.47	−6.62	−4.43	2.19	−0.001	0.976	−63.0
[PQ-PA]	−5.98	1.41	−6.65	−4.22	2.43	0.054	0.994	−92.6
[PQ-Pa]	−5.98	1.41	−6.47	−3.89	2.57	0.028	0.992	−89.9
[PQ-ACR]	−5.92	1.35	−6.48	−4.30	2.18	0.014	0.982	−79.2
[PQ-ACr]'	−5.92	1.35	−6.50	−4.38	2.11	0.023	0.981	−77.1
[PQ-CRS]	−5.76	1.19	−6.36	−4.21	2.15	0.060	1.007	−111.3
[PQ-ACN]	−5.71	1.14	−6.31	−4.43	1.88	0.005	0.983	−74.7
[PQ-aCn]'	−5.71	1.14	−6.25	−4.53	1.72	0.047	0.985	−75.8
[PQ-COR]	−5.70	1.13	−6.13	−4.21	1.92	0.031	1.010	−115.3
[PQ-PYR]	−5.58	1.01	−6.20	−4.20	2.00	0.068	0.992	−97.5
[PQ-MC]	−5.57	1.00	−6.27	−4.31	1.96	0.070	1.012	−94.0
[PQ-Mc]'	−5.57	1.00	−6.16	−4.23	1.92	0.071	1.008	−87.0

Table 1. Cont.

Molecule	$D_{E_{HOMO}}$	ΔE_{MO}	$CTC_{E_{HOMO}}$	$CTC_{E_{LUMO}}$	$\Delta^{CTC}E_{MO}$	q_{NPA}	q^*_{NPA}	ΔE_{ass}
[PQ-TPH]	−5.57	1.00	−6.17	−4.18	1.99	0.066	1.006	−104.8
[PQ-TPH]′	−5.57	1.00	−6.15	−4.21	1.94	0.065	1.005	−107.0
[PQ-AN]	−5.47	0.90	−6.12	−4.29	1.83	0.046	0.990	−82.3
[PQ-AZU]	−5.44	0.87	−6.02	−4.45	1.57	−0.004	0.969	−63.5
[PQ-AZU]′	−5.44	0.87	−6.27	−4.18	2.10	0.114	0.971	−73.3
[PQ-POR]	−5.39	0.82	−5.88	−4.07	1.82	0.077	1.033	−119.2
[PQ-TET]	−5.10	0.53	−5.70	−4.24	1.45	0.066	1.018	−106.1
[PQ-DBTTF]	−4.89	0.32	−5.53	−4.00	1.53	0.216	1.081	−124.0
[PQ-PEN]	−4.85	0.28	−5.45	−4.08	1.37	0.134	1.042	−118.0
[PQ-TTF]	−4.52	−0.05	−5.48	−4.03	1.45	0.240	1.089	−102.3
[PQ-DMPZ]	−4.39	−0.18	−5.26	−4.22	1.04	0.135	1.058	−107.5
[PQ-TMDA]	−4.37	−0.20	−5.38	−4.09	1.29	0.224	1.075	−104.3

2. Results and Discussion

2.1. Theoretical

The formation of charge transfer complexes is controlled by the energy difference (ΔE_{MO}) between the LUMO of the isolated acceptor (${}^A E_{LUMO}$) and the HOMO of the isolated donor (${}^D E_{HOMO}$) [3,13]. Since ${}^A E_{LUMO}$ is constant for all the considered CTCs and is equal to -4.57 eV, ΔE_{MO} depends only on ${}^D E_{HOMO}$ which varies from -6.97 to -4.37 eV for selected donors. Based on the ${}^D E_{HOMO}$ values we can expect an increase in donor properties in the following series: PD < BZ < QN < IQN < TPL < NA < PA < ACR < CRS < ACN < COR < PYR < MC < TPH < AN < AZU < POR < TET < DBTTF < PEN < TTF < DMPZ < TMDA (Table 1).

The most important structural features that determine electron donor properties of a molecule are the number and position of the condensed aromatic rings and also the presence of heteroatoms and functional groups. It is evident from Table 1 that donors become stronger as the number of aromatic rings grows. The ΔE_{MO} value decreases in the series of donors with linear arrangement of rings: BZ (2.39 eV), NA (1.47 eV), AN (0.90 eV), TET (0.53 eV), PEN (0.28 eV). The same goes for $\Delta^{CTC}E_{MO}$: the HOMO–LUMO energy difference in CTCs decreases from 3.10 eV to 1.37 eV for complexes of PQ with benzene and pentacene, respectively.

$\Delta^{CTC}E_{MO}$ values for anthracene [PQ-AN] (1.83 eV) and phenanthrene [PQ-PA] (2.43 eV)/[PQ-PA]′ (2.57 eV) complexes demonstrate that donors with a linear arrangement of aromatic rings are stronger than those with a non-linear arrangement. Similarly, $\Delta^{CTC}E_{MO}$ values increase when replacing tetracene [PQ-TET] (1.45 eV) to, tetraphene [PQ-TPH] (1.99 eV), pyrene [PQ-PYR] (2.00 eV), chrysene [PQ-CRS] (2.15 eV), or triphenylene [PQ-TPL] (2.37 eV). $\Delta^{CTC}E_{MO}$ for the pentacene complex [PQ-PEN] (1.37 eV) is lower than that for coronene [PO-COR] (1.92 eV) (Table 1).

Introduction of a nitrogen heteroatom into donor molecules leads to an increase of $\Delta^{CTC}E_{MO}$ values for the corresponding complexes, which points to a decrease of donor properties. The same trend for $\Delta^{CTC}E_{MO}$ holds true when changing BZ for PD, NA for QA/IQA, and AN for ACR (Table 1).

$\Delta^{CTC}E_{MO}$ values for complexes with acridine (1.88 and 1.72 eV) and azulene (1.57 and 2.10 eV) are found to be less than those of the complex with naphthalene (2.19 eV). Therefore, ACN and AZU are more active donors than NA. It is worth noting that the relative spatial arrangement of AZU and PQ molecules in CTCs (Figure S3) determines not only $\Delta^{CTC}E_{MO}$ values, but also the formation energies ΔE_{ass} (-63.5 and -73.3 kJ/mol) as well as the mean distance between donor and acceptor planes R (3.16 and 3.11 Å).

Substitution of benzene [PQ-BZ] for tetramethyl-p-phenylenediamine [PQ-TMDA] in the complex changes $\Delta^{CTC}E_{MO}$ from 3.10 to 1.29 eV. When TTF is replaced with DBTTF $\Delta^{CTC}E_{MO}$ of the corresponding complexes increases from 1.45 to 1.53 eV. The strongest

electron donor in the series considered in this work is DMPZ. $\Delta^{\text{CTC}}E_{\text{MO}}$ of [PQ-DMPZ] complex has the lowest value of 1.04 eV.

Donor and acceptor orbitals constitute the HOMO and LUMO in complexes (Figure S4). However, upon complexation their energy levels change: $^{\text{CTC}}E_{\text{HOMO}}$ lies below $^{\text{D}}E_{\text{HOMO}}$, while $^{\text{CTC}}E_{\text{LUMO}}$ is higher than $^{\text{A}}E_{\text{LUMO}}$ (Figure 2). For the CTCs having the highest degree of charge transfer in the series, namely, [PQ-TTF] and [PQ-TMDA], the magnitude of these changes reaches 1.50 eV and 1.49 eV, respectively. As a result, $\Delta^{\text{CTC}}E_{\text{MO}}$ values are significantly larger than the corresponding ΔE_{MO} but less than the HOMO-LUMO gaps of isolated PQ or the donors. Figure 2 illustrates this difference for CTCs of PQ with AN and TMDA: $\Delta^{\text{CTC}}E_{\text{MO}}$ values (1.83 and 1.29 eV) are smaller than the HOMO-LUMO gaps of PQ (3.37 eV), AN (3.56 eV) and TMDA (4.19 eV). The energy difference values ΔE_{MO} of isolated acceptor and donors in the series decrease from 2.40 to -0.20 eV (Table 1). Notably, $^{\text{D}}E_{\text{HOMO}}$ of the most pronounced donors, e.g., TTF, TMPZ, and TMDA, lies higher than $^{\text{A}}E_{\text{LUMO}}$ as graphically exemplified in Figure 2.

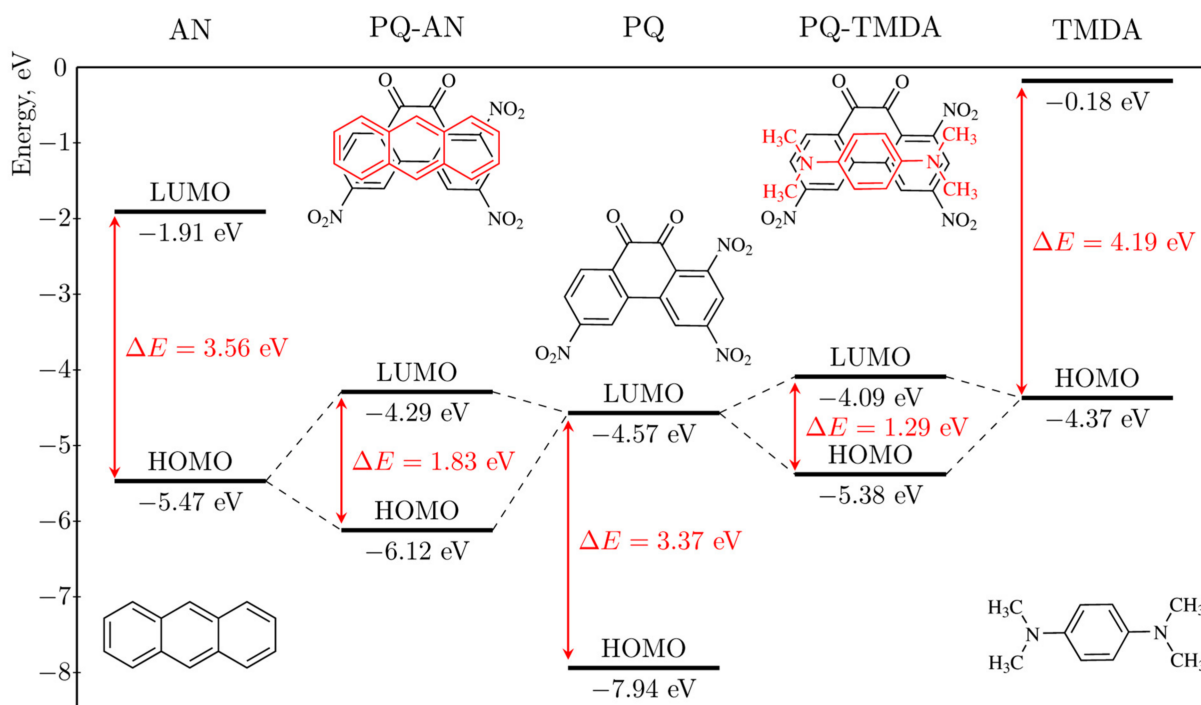


Figure 2. HOMO-LUMO energy levels for complexes of PQ with AN and TMDA according to DFT calculations.

The calculated wavelengths of electronic transitions based on the $\Delta^{\text{CTC}}E_{\text{MO}}$ values vary from 468 nm for the [PQ-QN]' complex, to 509 and 481 nm for the [PQ-PA] and [PQ-PA]' complexes, to 676 nm for the [PQ-AN] complex and further to 959 and 1186 nm for the [PQ-TMDA] and [PQ-DMPZ] complexes, respectively. Two sets of experimentally determined CT absorption bands for complexes [PQ-PA] and [PQ-AN] measured in CH_2Cl_2 and toluene are available in the literature. Solutions of complex with phenanthrene absorb at 490 and 495 nm [12], while [PQ-AN] spectra show peaks at 658 and 641 nm for dichloromethane and toluene, respectively [11]. The presence of the charge-transfer bands in the absorption spectra of the complexes is a reliable confirmation of the CTC formation. For a series of CTCs based on the same acceptor, the shift of charge-transfer bands to long wavelengths indicates an increase in donor power. According to this criterion, donor properties increase in the following sequence of molecules: QN, IQN, PA, TPL, NA, ACR, CRS, PYR, TPH, MC, COR, ACN, AZU, AN, POR, DBTTF, TET, TTF, PEN, TMDA, DMPZ.

The amounts of ground state charge transfer in CTCs q_{NPA} , calculated as the sum of NPA charges on donor atoms in CTC, is in the range from -0.004 to $0.249 e^-$. Assuming alternating molecular stacking in crystals, these CTCs can be classified as neutral and

mixed-valence CT solids [14]. Even a small charge transfer amount of 0.2 is enough for materials to exhibit conducting properties and neutral ionic phase transition in the mixed valent state [14]. For the first excited states the amounts of charge transfer q_{NPA}^* lie between 0.967 and 1.089 e^- (Table 1). This indicates that the electron transitions upon excitation in the CTCs are mainly associated with the transfer of electron density from the donor to the acceptor atoms.

Absolute values of the calculated association energies ΔE_{ass} increase as the π -conjugated system grows. In the series BZ, NA, AN, TET, and PEN ΔE_{ass} values are -47.0 , -63.5 , -82.3 , -106.1 , and -118.0 kJ/mol, respectively. The stability of CTCs with TTF, TMDA, DMPZ, POR, and DBTTF is determined not by the size of molecule, but by the presence of heteroatoms (Table 1).

The calculated intermolecular separation distances (R) in CTCs lie in the range from 2.87 to 3.25 Å. The complexes with the lowest distance values exhibit substantial deviation from a planar structure (Figure S5). The calculated R for [PQ-AN] complex (3.24 Å) agrees with the interplanar distance of the X-ray structure (3.49 ± 0.26 Å). The bond lengths of [PQ-AN] predicted by DFT are close to those of both calculated structures of isolated PQ and AN and the X-ray structure (Table 2).

Table S1 demonstrates the NPA charges on atoms of complex [PA-AN] and isolated molecules PQ and AN in both ground and first excited states. In the ground state of [PQ-AN] complex the amount of charge transferred from AN to PQ equals 0.046 e^- . Interestingly, this value hides the fact that AN carbon atoms gain $-0.062 e^-$ while hydrogen atoms lose 0.111 e^- when the complex forms. At the same time oxygen and nitrogen atoms are the acceptor centers of PQ.

Upon excitation the charge on the donor increases to 0.990 e^- indicating the formation of $[D^+A^-]$ complex. This is accompanied by the electron density transfer from AN carbon atoms to PQ oxygen and nitrogen atoms (0.369 e^-) and C-atoms (0.624 e^-).

Table 2. Bond lengths d (Å) and valence angles ω (deg.) of complex I (X-ray diffraction data), complex [PQ-AN] and isolated PQ and AN molecules (DFT calculations). Atom numbering scheme is given in Figure 3.

Bond	d			Angle	ω		
	I	[PQ-AN]	PQ, AN		I	[PQ-AN]	PQ, AN
O ⁵ -C ⁵	1.2103(13)	1.208	1.207	O ¹ -N ¹ -O ²	124.64(10)	125.5	125.9
O ⁶ -C ⁶	1.2135(13)	1.211	1.209	O ² -N ¹ -C ²	117.20(9)	117.1	117.0
O ¹ -N ¹	1.2258(13)	1.219	1.217	O ¹ -N ¹ -C ²	118.16(9)	117.4	117.1
O ² -N ¹	1.2257(13)	1.218	1.217	O ³ -N ² -O ⁴	125.46(10)	126.7	127.2
O ³ -N ²	1.2198(13)	1.214	1.215	O ⁴ -N ² -C ⁴	117.13(9)	116.4	116.4
O ⁴ -N ²	1.2211(13)	1.217	1.214	O ³ -N ² -C ⁴	117.32(9)	116.7	116.3
O ⁷ -N ³	1.2289(13)	1.220	1.218	O ⁷ -N ³ -O ⁸	123.79(10)	125.2	125.6
O ⁸ -N ³	1.2264(13)	1.219	1.217	O ⁷ -N ³ -C ⁹	118.31(9)	117.4	117.3
N ¹ -C ²	1.4712(14)	1.479	1.485	O ⁸ -N ³ -C ⁹	117.89(9)	117.4	117.1
N ² -C ⁴	1.4791(13)	1.480	1.482	O ⁵ -C ⁵ -C ^{4A}	122.52(10)	123.0	122.8
N ³ -C ⁹	1.4717(13)	1.477	1.484	O ⁵ -C ⁵ -C ⁶	119.50(10)	120.0	119.8
C ⁵ -C ⁶	1.5379(15)	1.537	1.540	C ^{4A} -C ⁵ -C ⁶	117.91(9)	117.0	117.3
C ^{10A} -C ^{10B}	1.4819(15)	1.480	1.484	O ⁶ -C ⁶ -C ^{6A}	123.53(10)	123.3	123.2
C ¹¹ -C ¹²	1.3606(18)	1.373	1.373	O ⁶ -C ⁶ -C ⁵	118.92(10)	119.6	119.5
C ¹² -C ¹³	1.4213(17)	1.427	1.428	C ^{6A} -C ⁶ -C ⁵	117.54(9)	117.1	117.2
C ¹¹ -C ^{14B}	1.4303(17)	1.431	1.431	C ³ -C ⁴ -N ²	115.79(9)	115.7	115.9
C ^{14A} -C ¹⁵	1.3968(17)	1.403	1.402	C ^{4A} -C ⁴ -N ²	120.83(9)	121.4	121.4
C ^{14A} -C ^{14B}	1.4400(15)	1.446	1.446	C ¹² -C ¹¹ -C ^{14B}	120.73(11)	120.8	121.0

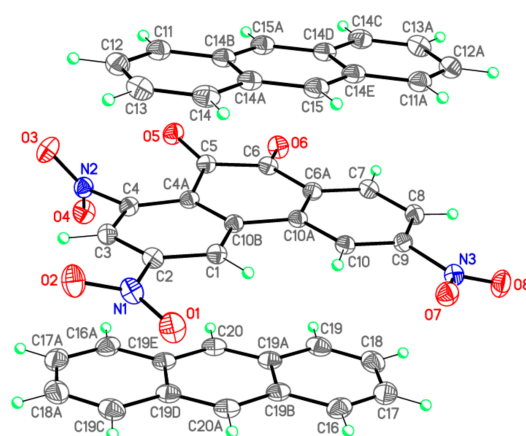


Figure 3. X-ray crystallographic structure of PQ and AN in complex I.

2.2. Experimental

Dark green single prism-shaped crystals of [PQ-AN] complex (I) were grown by slow evaporation from equimolar solution of PQ and AN in CH_2Cl_2 . The X-ray diffraction study confirmed the 1:1 ratio of PQ and AN in complex I and revealed the monoclinic structure (space group $P2_1/c$).

The molecular structure of PQ was determined for the first time, although in a complex with AN. It is interesting to discuss and compare the main geometric features of PQ and 2,4,7-trinitro-9,10-phenanthrenequinone (TNPQ), especially in complexes with AN (II [11]) and PA (III [12]).

The C=O bond lengths in I (1.2103(13) and 1.2135(13) Å, Table 2, Figure 3) do not differ from those in II (1.211(2) and 1.217(2) Å) [11] and III (1.211(2) and 1.216(2) Å) [12]. The bond C⁵–C⁶ in I (1.5379(15) Å) is significantly longer than the standard single bond of C(*sp*²)–C(*sp*²) type (1.479 Å) [15]. This deviation is determined by anti-bonding interactions of oxygen atoms in *o*-quinones as was shown earlier in II (1.528(2) Å) [11] and III (1.526(2) Å) [12]. Valence angles of C⁵ and C⁶ in I have values close to those of II and III. In complex I atoms O⁵ and O⁶ are found to deviate notably from the plane of the central ring of PQ (torsion angle O⁵–C⁵–C⁶–O⁶ is 15.54(16)°), which is different from TNPQ where atoms O⁵ and O⁶ lie on the plane of the central ring (0.4(2)° for II [11] and 0.8(2)° for III [12]).

The main structural features of NO₂ groups in I (Table 2), II [11], and III [12] differ only slightly and are close to the average values [16]: the N–O bond lengths in I are in the range from 1.2198(13) to 1.2289(13) Å and the O–N–O valence angles are from 123.79(10)° to 125.46(10)°. The nitro groups in structure I at atoms C², C⁴, and C⁹ are rotated out of the aromatic plane by 16.84(13), 62.75(13) and 13.56(12)°, respectively, which significantly distinguishes them from similar values at atoms C¹, C³, and C⁸ in II (69.02(19), 0.25(18), and 19.93(18)°) [11] and III (73.8(2), 1.35(15), and 0.95(15)°) [12]. Unlike structures II and III, where the greatest rotation angle was observed in the NO₂ group at the C¹ atom, experiencing significant steric repulsion from atoms C¹⁰ and H¹⁰, in structure I steric difficulties arise between the nitro group at the atom C⁴ and the carbonyl group O⁵–C⁵, which causes a ~63° rotation of the NO₂ group and a significant non-planarity of the carbonyl. It should be noted that the C–N bonds near the heavily rotated nitro groups are somewhat elongated relative to other similar bonds: N²–C⁴ 1.4791(13) Å in I (Table 2), N¹–C¹ 1.480(2) Å in II [11], and N¹–C¹ 1.483(2) Å in III [12].

The AN molecule in complex I has C–C bond lengths in the range from 1.359(2) to 1.4400(15) Å and valence angles between 118.32(12)–122.62(11)°, which match with the corresponding values in II (bonds from 1.360(3) to 1.443(2) Å and angles within 118.38(14)–122.50(15)° [11]), in the free AN molecule [15] and in its CTC with 2,3,5,6-tetrachloro-1,4-dicyanobenzene [17].

In crystal I, the molecules of the acceptor PQ and the donor AN are arranged parallel to each other and form stacks of mixed type $\{\dots[\text{A-D}]\dots[\text{A-D}']\dots\}_\infty$ along the crystallographic

axis *a* (Figure 4). Every second PQ molecule in the stack is rotated in a plane by 180° relative to the previous one (A and A'), which was observed for TNPQ molecules in II [11]. The AN molecules in I are displaced relative to each other (D and D') only slightly and their central ring practically overlaps, which distinguishes them significantly from II, where the AN molecules are rotated by 60° relative to each other [11]. As a result of this mutual arrangement of the molecules PQ and AN in I, peculiar triads [D-A]···[D-]' and [D-A]'···[D-] are formed, in which the π systems of the donor and the acceptor overlap almost to the same degree (Figure 4).

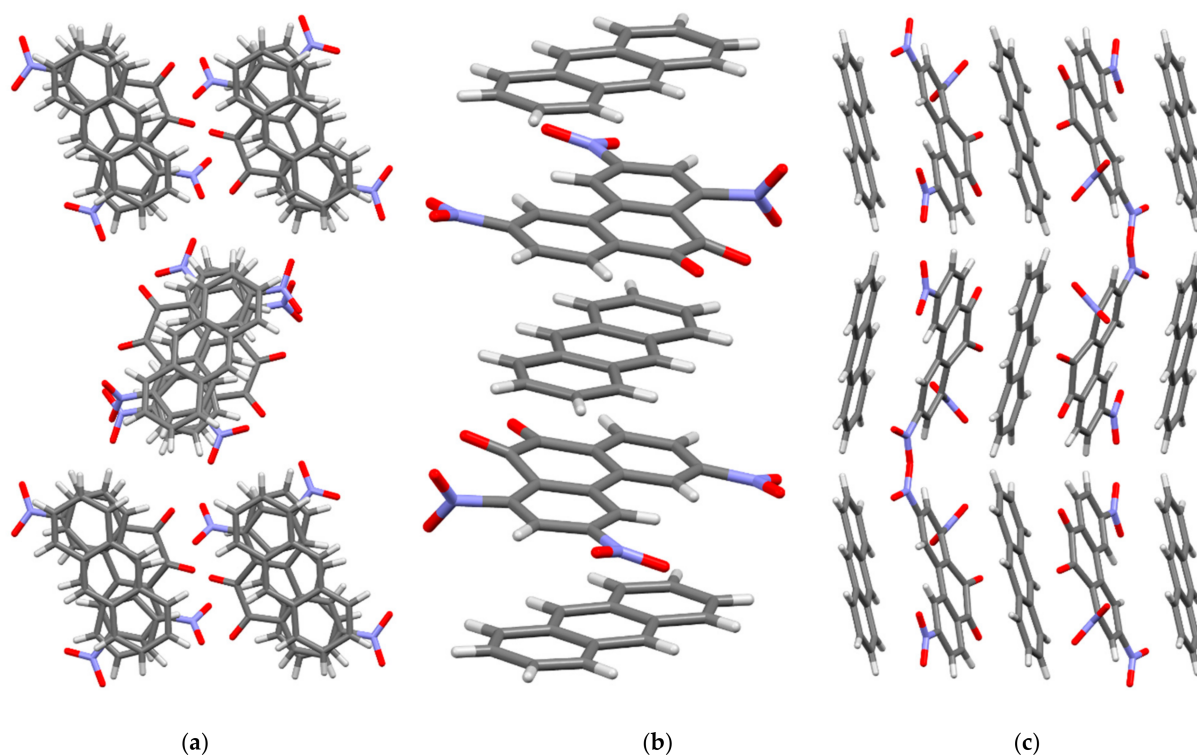


Figure 4. Crystal structure of complex I. (a) View along crystallographic *a* axis; (b) view along crystallographic *b* axis; (c) view along crystallographic *c* axis.

In I, the PQ and AN molecules form two types of shortened contacts which are less than the sum of the van der Waals radii (Table S2). [A-D] and, [D-A]' contacts are found in the same stack while A···D and A···A' contacts are between the adjacent stacks. In one stack, each acceptor molecule establishes six C···C contacts with molecules D and D' in the range from 3.263(2) to 3.363(2) Å, which may indicate strong π - π interactions between the molecules. The molecules D and D' form a different number of shortened C···C contacts in the stack: each D molecule has four C···C contacts with acceptor molecules A and A', while each D' has only two such contacts.

The average interplanar distances D···A in I are about 3.434(5) Å, which is close to those in CTCs of AN with 2,3,5,6-tetrachloro-1,4-dicyanobenzene (3.427(3) Å) [17] or with 2,3,5,6-tetrafluoro-7,7,8,8-tetracyanoquinodimethane (3.379(2) Å) [18]. The calculated charge transfer values for the CTCs [PQ-AN] (0.046 e⁻) (Table 1) and [TNPQ-AN] (0.091 e⁻) [11] are consistent with the interplanar distances.

Each PQ molecule in I interacts with AN and PQ molecules from adjacent stacks via O···H-C shortened contacts in the range of 2.45–2.64 Å. There are also O···C contacts between the PQ molecules from adjacent stacks—from 2.921(2) to 3.097(2) Å (Table S2). The presence of such a significant number of various intermolecular interactions in I, the number of which for each PQ molecule reaches twenty-five, and the observed geometric characteristics of PQ can be due to its high acceptor capacity.

3. Materials and Methods

3.1. Synthesis

1,3,6-trinitro-9,10-phenathrenequinone (PQ, melting point 261–263 °C) was obtained by nitration and subsequent decomposition of 9,10-sulfonyldioxyphenanthrene in concentrated nitric acid ($d = 1.51$) [19]. Pure-grade anthracene was used without additional purification. The solvent, namely, pure-grade CH_2Cl_2 was purified by standard methods. To obtain CTC in the crystalline state, the solutions of acceptor (PQ, 0.2 mmol in 12 mL of CH_2Cl_2) and donor (AN, 0.2 mmol in 5 mL of CH_2Cl_2) were mixed in equimolar amounts. Single crystals of the [PQ-AN] complex suitable for the X-ray diffraction studies were grown by slow evaporation of the solvent.

3.2. X-ray Crystallography and Structure Refinement

The X-ray diffraction study of [PQ-AN] complex was carried out at the “BELOK” beamline of the Kurchatov Institute Synchrotron Radiation Source. The parameters of the unit cell and the reflection intensities were measured using a Rayonix SX165 CCD two coordinate detector ($\lambda = 0.79272 \text{ \AA}$, φ -scanning in 1.0° steps) (Rayonix LLC, 1880 Oak Ave UNIT 120, Evanston, IL 60201, USA). The structure was solved by direct methods and refined by the full-matrix least squares technique on F^2 with anisotropic displacement parameters for all non-hydrogen atoms using the iMOSFLM (CCP4) [20], SCALA [21], and SHELXL [22] programs. All hydrogen atoms were placed in calculated positions and included in the refinement within the riding model with fixed isotropic displacement parameters $U_{\text{iso}}(\text{H}) = 1.5U_{\text{eq}}(\text{O})$, $1.2U_{\text{eq}}(\text{N})$, and $1.2U_{\text{eq}}(\text{C})$. The crystallographic data as well as the experimental and refinement parameters are summarized in Table 3. Crystallographic data is available online at the Cambridge Crystallographic Data Centre (CCDC 2099997).

Table 3. Summary of crystallographic experiment data and structure refinement parameters for I.

Compound	I
CCDC	2099997
Formula	$\text{C}_{14}\text{H}_5\text{N}_3\text{O}_8 \cdot \text{C}_{14}\text{H}_{10}$
Crystal system	Monoclinic
Space group	$P2_1/c$
Z	4
$a, b, c, \text{ \AA}$	14.2721(14), 19.479(2), 8.1900(9)
$\alpha, \beta, \gamma, \text{ deg}$	90, 99.041(8), 90
$V, \text{ \AA}^3$	2248.6(4)
$D_x, \text{ g/cm}^3$	1.540
Radiation, $\lambda, \text{ \AA}$	Synchrotron, 0.79272
$\mu, \text{ mm}^{-1}$	0.147
T, K	100(2)
Specimen size, mm	$0.18 \times 0.15 \times 0.03$
Absorption correction	Semi-empirical
$T_{\text{min}}/T_{\text{max}}$	0.966/0.987
$\theta_{\text{max}}, \text{ deg}$	30.95
Limits of h, k, l	$-15 \leq h \leq 18; -25 \leq k \leq 18; -10 \leq l \leq 10;$
Number of reflections: measured/independent (N_1); observed with $I > 2\sigma(I)$ (N_2)	13943/5033 4596
R_{int}	0.0276
Number of parameters	353
Extinction coefficient	0.029(3)
R_1/wR_2 by N_1	0.0404/0.0975
R_1/wR_2 by N_2	0.0373/0.0950
S	1.023
$\Delta\rho_{\text{min}}/\Delta\rho_{\text{max}}, \text{ e \AA}^{-3}$	$-0.220/0.261$

3.3. Quantum Chemical Calculations

Quantum chemical simulation of the electronic structure of donor, acceptor, and CTC molecules was performed in the framework of the density functional theory using the B3LYP hybrid functional and the def2-SV(P) basis set. TDDFT methodology was used to explore the low-lying excited states. The Boys–Bernardi method was used for BSSE correction [23]. All D4 dispersion correction was used in all calculations [24]. The amount of charge transfer from a donor to an acceptor was calculated using the natural populations analysis (NPA) [25] as the difference between the sum of charges on the acceptor atoms in free state and in complex for both the ground ($\Delta q_{\text{NPA}}, e^-$) and first excited ($\Delta q^*_{\text{NPA}}, e^-$) states. The CTC association energies are defined as follows:

$$\Delta E_{\text{ass}} = {}^{\text{CTC}}E_{\text{tot}} - {}^{\text{A}}E_{\text{tot}} - {}^{\text{D}}E_{\text{tot}}$$

where ${}^{\text{CTC}}E_{\text{tot}}$, ${}^{\text{A}}E_{\text{tot}}$ and ${}^{\text{D}}E_{\text{tot}}$ are total energies (in kJ/mol) of the CTC, acceptor, and donor, respectively. All the calculations were performed using the Firefly 8.20 software package [26].

4. Conclusions

In this study we explored a series of 23 charge transfer complexes based on 1,3,6-trinitro-9,10-phenanthrenequinone and different electron donors by means of density functional theory. Complexes with dibenzotetrathiafulvalene, pentacene, tetrathiafulvalene, 5,10-dimethylphenazine, and tetramethyl-p-phenylenediamine were shown to be in a mixed-valence state with a ground state charge transfer degree of 0.134–0.240 e^- . A charge transfer complex with anthracene was synthesized, isolated as a single crystal, and the structure determined by X-ray diffraction experiment. Geometric and electronic structure features and their influence on the charge transfer properties of the complexes are discussed.

Supplementary Materials: The following are available online. Figure S1: Chemical structure depiction of PQ and 23 donors used in this work, Figure S2: Configurations of charge transfer complexes considered in this work, Figure S3: DFT optimized molecular structure of complexes: (a) [PQ-AZU] and (b) [PQ-AZu]', Figure S4: Electron density corresponding to (a) HOMO and (b) LUMO of [PQ-AN] complex, Figure S5: DFT optimized molecular structure of complexes: (a) [PQ-DBTTF] ($R = 2.87 \text{ \AA}$) and (b) [PQ-DMPZ] ($R = 3.02 \text{ \AA}$), Table S1: Calculated NPA partial charges on atoms of complex [PQ-AN] in ground and first excited ([PQ-AN]*) states and of isolated PQ and AN molecules, Table S2: Selected shortened contacts d (\AA) between PQ and AN in complex I.

Author Contributions: Conceptualization, R.L.; methodology, R.L., M.R., V.D. and P.S.; validation, R.L., M.R. and P.S.; formal analysis, M.R.; investigation, R.L., M.R., P.S., P.D. and V.K.; writing—original draft preparation, R.L., M.R. and P.S. writing—review and editing, R.L., M.R. and P.S.; visualization, R.L., M.R. and P.S. supervision, R.L.; project administration, R.L.; funding acquisition, R.L. All authors have read and agreed to the published version of the manuscript.

Funding: This paper was supported by the RUDN University Strategic Academic Leadership Program.

Data Availability Statement: Not applicable.

Conflicts of Interest: The authors declare no conflict of interest.

Sample Availability: Samples of the compounds are not available from the authors.

Abbreviations

ΔE_{MO}	the energy difference between ${}^{\text{A}}E_{\text{LUMO}}$ and ${}^{\text{D}}E_{\text{HOMO}}$
${}^{\text{D}}E_{\text{HOMO}}$	energy level of the HOMO of isolated donor molecule
${}^{\text{A}}E_{\text{LUMO}}$	energy level of the LUMO of isolated acceptor molecule
$\Delta{}^{\text{CTC}}E_{\text{MO}}$	the energy difference between ${}^{\text{CTC}}E_{\text{LUMO}}$ and ${}^{\text{CTC}}E_{\text{HOMO}}$
${}^{\text{CTC}}E_{\text{HOMO}}$	energy level of the HOMO of complex
${}^{\text{CTC}}E_{\text{LUMO}}$	energy level of the LUMO of complex
q_{NPA}	partial NPA charges in the ground state
q^*_{NPA}	partial NPA charges in the first excited state
ΔE_{ass}	energy of association of donor and acceptor
A	acceptor
ACN	acenaphthene
ACR	acridine
AN	anthracene
AZU	azulene
BZ	benzene
COR	coronene
CRS	chrysene
CTCs	charge transfer complexes
D	donor
DBTTF	dibenzotetrathiafulvalene
DFT	density functional theory
DMPZ	5,10-dimethylphenazine
HOMO	highest occupied molecular orbital
IQN	isoquinoline
LUMO	lowest unoccupied molecular orbital
MC	9-methylcarbazole
NA	naphthalene
PA	phenanthrene
PD	pyridine
PEN	pentacene
POR	porphyrin
PQ	1,3,6-trinitro-9,10-phenanthrenequinone
PYR	pyrene
QN	quinoline
TET	tetracene
TMDA	N,N,N',N'-tetramethyl-p-phenylenediamine
TPH	tetraphene
TPL	triphenylene
TTF	tetrathiafulvalene

References

- Pavelyev, V.G.; Parashchuk, O.D.; Krompiec, M.; Orekhova, T.V.; Perepichka, I.F.; Van Loosdrecht, P.H.M.; Paraschuk, D.Y.; Pshenichnikov, M.S. Charge transfer dynamics in donor-acceptor complexes between a conjugated polymer and fluorene acceptors. *J. Phys. Chem. C* **2014**, *118*, 30291–30301. [[CrossRef](#)]
- Al Kobaisi, M.; Bhosale, R.S.; El-Khouly, M.E.; La, D.D.; Padghan, S.D.; Bhosale, S.V.; Jones, L.A.; Antolasic, F.; Fukuzumi, S.; Bhosale, S.V. The sensitivity of donor – acceptor charge transfer to molecular geometry in DAN–NDI based supramolecular flower-like self-assemblies. *Sci. Rep.* **2017**, *7*, 16501. [[CrossRef](#)] [[PubMed](#)]
- Hu, P.; Du, K.; Wei, F.; Jiang, H.; Kloc, C. Crystal Growth, HOMO–LUMO Engineering, and Charge Transfer Degree in Perylene- F_x TCNQ ($x = 1, 2, 4$) Organic Charge Transfer Binary Compounds. *Cryst. Growth Des.* **2016**, *16*, 3019–3027. [[CrossRef](#)]
- Singh, M.; Chopra, D. Diversity in Mechanical Response in Donor–Acceptor Coupled Cocrystal Stoichiomorphs Based on Pyrene and 1,8-Dinitroanthraquinone Systems. *Cryst. Growth Des.* **2018**, *18*, 6670–6680. [[CrossRef](#)]
- Averkiev, B.; Isaac, R.; Jucov, E.V.; Khrustalev, V.N.; Kloc, C.; McNeil, L.E.; Timofeeva, T.V. Evidence of Low-Temperature Phase Transition in Tetracene–Tetracyanoquinodimethane Complex. *Cryst. Growth Des.* **2018**, *18*, 4095–4102. [[CrossRef](#)]
- Henderson, J.; Masino, M.; Hatcher, L.E.; Kociok-Köhn, G.; Salzillo, T.; Brillante, A.; Raithby, P.R.; Girlando, A.; Da Como, E. New Polymorphs of Perylene:Tetracyanoquinodimethane Charge Transfer Cocrystals. *Cryst. Growth Des.* **2018**, *18*, 2003–2009. [[CrossRef](#)]

7. Starodub, V.A.; Starodub, T.N. Radical anion salts and charge transfer complexes based on tetracyanoquinodimethane and other strong π -electron acceptors. *Russ. Chem. Rev.* **2014**, *83*, 391. [CrossRef]
8. Wang, W.; Luo, L.; Sheng, P.; Zhang, J.; Zhang, Q. Multifunctional Features of Organic Charge-Transfer Complexes: Advances and Perspectives. *Chem.-A Eur. J.* **2021**, *27*, 464–490. [CrossRef] [PubMed]
9. Cui, Z.; Aquino, A.J.A.; Sue, A.C.-H.; Lischka, H. Analysis of charge transfer transitions in stacked π -electron donor–acceptor complexes. *Phys. Chem. Chem. Phys.* **2018**, *20*, 26957–26967. [CrossRef] [PubMed]
10. Mukherjee, T.K. Electron affinities of polynuclear acceptors. Dinitro- and trinitrophenanthrenequinones. *J. Phys. Chem.* **1967**, *71*, 2277–2282. [CrossRef]
11. Linko, R.V.; Ryabov, M.A.; Strashnov, P.V.; Polyanskaya, N.A.; Davydov, V.V.; Dorovatovskii, P.V.; Lin'ko, I.V.; Khrustalev, V.N. Charge transfer complexes of nitro derivatives of 9,10-phenanthrenequinone with anthracene. crystal and molecular structures of the (1:1) complex of 2,4,7-trinitro- 9,10-phenanthrenequinone with anthracene. *J. Struct. Chem.* **2021**, *62*, 137–146. [CrossRef]
12. Linko, R.V.; Ryabov, M.A.; Strashnov, P.V.; Polyanskaya, N.A.; Davydov, V.V.; Dorovatovskii, P.V.; Khrustalev, V.N. Quantum-Chemical Simulation of the Structure of Charge-Transfer Complexes of 9,10-Phenanthrenequinone Nitro-Derivatives with Phenanthrene. Crystal and Molecular Structure of 1:1 Complex of 2,4,7-Trinitro–9,10-phenanthrenequinone with Phenanthrene. *Russ. J. Gen. Chem.* **2020**, *90*, 1869–1877. [CrossRef]
13. Winget, P.; Brédas, J.-L. Ground-State Electronic Structure in Charge-Transfer Complexes Based on Carbazole and Diarylamine Donors. *J. Phys. Chem. C* **2011**, *115*, 10823–10835. [CrossRef]
14. Saito, G.; Murata, T. Mixed valency in organic charge transfer complexes. *Philos. Trans. R. Soc. A Math. Phys. Eng. Sci.* **2008**, *366*, 139–150. [CrossRef]
15. Sinclair, V.C.; Robertson, J.M.; McL Mathieson, A. The crystal and molecular structure of anthracene. II. Structure investigation by the triple Fourier series method. *Acta Crystallogr.* **1950**, *3*, 251. [CrossRef]
16. Sadova, N.I.; Vilkov, L.V. The Molecular Geometry of Nitro-compounds. *Russ. Chem. Rev.* **1982**, *51*, 87–105. [CrossRef]
17. Britton, D. 2,3,5,6-Tetrachloro–1,4-dicyanobenzene–anthracene (1/1). *Acta Crystallogr. Sect. E Struct. Rep. Online* **2005**, *61*, o1707–o1708. [CrossRef]
18. Hu, P.; Li, H.; Li, Y.; Jiang, H.; Kloc, C. Single-crystal growth, structures, charge transfer and transport properties of anthracene-F₄ TCNQ and tetracene-F₄ TCNQ charge-transfer compounds. *CrystEngComm* **2017**, *19*, 618–624. [CrossRef]
19. Andrievskii, A.M.; Linko, R.V.; Grachev, M.K. Synthesis and reactions of trinitro–9,10-phenanthrenequinone derivatives. *Russ. J. Org. Chem.* **2013**, *49*, 1025–1030. [CrossRef]
20. Batty, T.G.G.; Kontogiannis, L.; Johnson, O.; Powell, H.R.; Leslie, A.G.W. *iMOSFLM*: A new graphical interface for diffraction-image processing with *MOSFLM*. *Acta Crystallogr. Sect. D Biol. Crystallogr.* **2011**, *67*, 271–281. [CrossRef]
21. Evans, P. Scaling and assessment of data quality. *Acta Crystallogr. Sect. D Biol. Crystallogr.* **2006**, *62*, 72–82. [CrossRef]
22. Sheldrick, G.M. Crystal structure refinement with *SHELXL*. *Acta Crystallogr. Sect. C Struct. Chem.* **2015**, *71*, 3–8. [CrossRef]
23. Boys, S.F.; Bernardi, F. The calculation of small molecular interactions by the differences of separate total energies. Some procedures with reduced errors. *Mol. Phys.* **1970**, *19*, 553–566. [CrossRef]
24. Caldeweyher, E.; Bannwarth, C.; Grimme, S. Extension of the D3 dispersion coefficient model. *J. Chem. Phys.* **2017**, *147*, 034112. [CrossRef]
25. Glendening, E.D.; Badenhoop, J.K.; Reed, A.E.; Carpenter, J.E.; Bohmann, J.A.; Morales, C.M.; Weinhold, F. *NBO 5.0*; Theoretical Chemistry Institute, University of Wisconsin: Madison, WI, USA, 2004.
26. Granovsky, A.A. FireFly Version 8.20. Available online: <http://classic.chem.msu.su/gran/firefly/index.html> (accessed on 20 May 1997).